Real-time multidimensional NMR follows RNA folding with second resolution

Mi-Kyung Lee[a,1], Maayan Gal[b,1], Lucio Frydman[b,2], and Gabriele Varani[a,c,2]

[a]Department of Chemistry, University of Washington, Box 351700, Seattle WA 98195; [b]Department of Chemical Physics, Weizmann Institute of Science, 76100 Rehovot, Israel; and [c]Department of Biochemistry, University of Washington, Box 357350, Seattle, WA 98195

Edited by Ignacio Tinoco, University of California, Berkeley, Berkeley, CA, and approved April 6, 2010 (received for review January 29, 2010)

Conformational transitions and structural rearrangements are central to the function of many RNAs yet remain poorly understood. We have used ultrafast multidimensional NMR techniques to monitor the adenine-induced folding of an adenine-sensing riboswitch in real time, with nucleotide-resolved resolution. By following changes in 2D spectra at rates of approximately 0.5 Hz, we identify distinct steps associated with the ligand-induced folding of the riboswitch. Following recognition of the ligand, long range loop-loop interactions form and are then progressively stabilized before the formation of a fully stable complex over approximately 2–3 minutes. The application of these ultrafast multidimensional NMR methods provides the opportunity to determine the structure of RNA folding intermediates and conformational trajectories.

dynamics | riboswitches | ultrafast NMR | conformational transition

Riboswitches are genetic control elements found in untranslated regions of prokaryotic and, less often, eukaryotic mRNAs (1). Their function in gene regulation depends on their ability to change structure in response to ligand binding, a property shared with many other functional RNAs (2, 3). They are composed of a ligand-binding domain that is very well conserved to specifically recognize the target metabolite and an expression platform whose structure is altered when the ligand-binding domain is occupied. The change in structure in the expression platform modulates transcription termination or translation initiation in response to changes in metabolite concentration (4, 5). While the structural basis for ligand recognition is known for many riboswitches, how the associated conformational changes occur is much less well understood. Yet the function of the riboswitches depends on their ability to change structure in response to ligand binding, and indeed the kinetics of ligand binding can affect gene regulation (6–8).

Purine-sensing riboswitches have been studied with particular intensity because they represent ideal model systems to understand ligand recognition and riboswitch function. The structure of the adenine-sensing riboswitch aptamer domain bound to adenine has been determined by X-ray crystallography (9, 10) and studied extensively by NMR as well (11–13). These studies have shown how a single nucleotide can switch the specificity from adenine to guanine and revealed the architecture of the riboswitch. The structure is composed of three helices emanating from the junction; two hairpin loops capping helices 2 and 3 form a tuning fork-like architecture in the presence of the ligand (Fig. 1), while the three-way junction is responsible for direct adenine recognition. The structure of free adenine-sensing riboswitch aptamer is much more flexible, preventing so far a detailed structural characterization.

Single molecule techniques have been applied to studying the time-dependent folding of the purine riboswitch while actively transcribed on the RNA polymerase (14, 15). These force spectroscopy studies have revealed multiple folding steps associated with formation of secondary and tertiary contacts, but this otherwise powerful technique lacks atomic resolution. One-dimensional NMR has also been employed, together with rapid mixing techniques, to follow the ligand-induced conformational change of the purine-sensing riboswitch (12), but only some resonances can be individually resolved in 1D spectra of large RNAs. Obviously, the application of multidimensional NMR methods would greatly improve our ability to follow these conformational transitions in real time and with atomic resolution, provided fast enough data collection could be achieved.

Advances in fast data collection in NMR spectroscopy (16, 17) suggested that it may be possible to monitor conformational changes of riboswitches, which occur with relatively slow time course of seconds (8, 12), using real-time multidimensional NMR. Here we report the successful collection of 2D ultraSOFAST NMR spectra (18), recorded at repetition rates of about 0.5 Hz, to follow the complete conformational change from ligand-free to ligand-bound form of the adenine riboswitch. Interpretation of these time-resolved HMQC spectra identifies multiple folding intermediates sampled by the riboswitch at nucleotide resolution and with a real-time resolution approaching 1 sec.

Results

NMR Studies the Ligand-Free and Ligand-Bound Forms of the Adenine-Sensing Riboswitch. The *add* adenine-sensing riboswitch aptamer domain contains 71 nucleotides. The NOESY spectrum of this RNA is severely overlapped and broad, because of the slow tumbling time. In order to obtain the spectral assignments needed for our subsequent work, the RNA was per-deuterated at the H5, H3′, H4′, and H5′-H5′′ positions, while retaining full protonation at the H6/H8/H2, H1′, and H2′ positions (19); representative spectra of the resulting constructs are shown in *SI Text*. In the fingerprint region of the nonexchangeable NOESY spectrum, most residues in the three helices (called P1, P2, and P3, Fig. 1) show sequential connectivities indicating that the residues are stacked on each other. However, the junctions and loops are disconnected in the sequential NOE walk. In ^{1}H, ^{15}N-HSQC's or NOESY spectra, we cannot observe the A19-U77, U20-A76, and A21-U75 base pairs within the P1 helix. Sequential NOE interactions, however, connect A19 to A21 and U75 to U77. Evidence for three putative base pairs within P2 (U31-U39, A30-U40, and A29-U41) could not be found either, even if sequential NOEs are consistent with a stacked helical conformation for these nucleotides. These observations suggest that helices 1 and 2 are only partially stable, perhaps because of structural flexibility of the J1-2 and J3-1 junctions.

In order to reach the bound form of the riboswitch, $MgCl_2$ was titrated into a solution containing equivalent amounts of

Author contributions: L.F. and G.V. designed research; M.-K.L. and M.G. performed research; M.-K.L., M.G., L.F., and G.V. analyzed data; and M.-K.L., M.G., L.F., and G.V. wrote the paper.

The authors declare no conflict of interest.

This article is a PNAS Direct Submission.

[1]M.-K.L and M.G. contributed equally to this work.

[2]To whom correspondence may be addressed. E-mail: lucio.frydman@weizmann.ac.il and varani@chem.washington.edu.

This article contains supporting information online at www.pnas.org/lookup/suppl/doi:10.1073/pnas.1001195107/-/DCSupplemental.

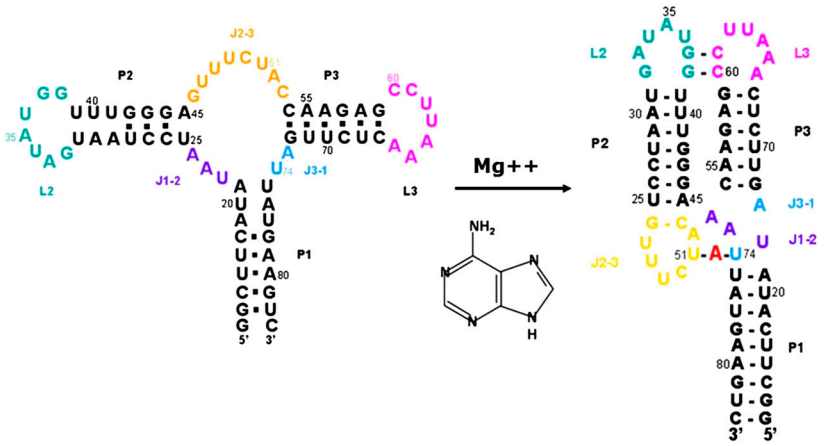

Fig. 1. Sequence and secondary structures of the ligand-free and ligand-bound adenine-sensing riboswitch ligand-binding domain of the *add* A-riboswitch from *Vibrio vulnificus* (10). The secondary structure of the free riboswitch is based on NMR data (11, 12), as well as the assignments reported in this study.

nucleotide and RNA, and 2D ^{1}H, ^{15}N HSQC spectra were recorded. Optimal conditions were found to contain a 10-fold excess of Mg^{2+}. In the absence of adenine, the Mg^{2+} ions induces only subtle chemical shift changes in the imino protons of the riboswitch, indicating that it does not change the structure of the riboswitch ligand-binding domain; however, binding of adenine to the riboswitch was not completed without Mg^{2+} ions. In the ^{1}H, ^{15}N-HSQC spectrum of the bound RNA (Fig. 2), most imino proton peaks in the three helices were observed, indicating that all helices are stabilized by ligand binding; new imino proton signals corresponding to the three-helix junctions appear as well. The structure demonstrates that adenine forms a Watson–Crick base pair with U74 and interacts with U47, U51, and U22 (9, 10). Consistent with previous studies (11), the H_2O NOESY of the

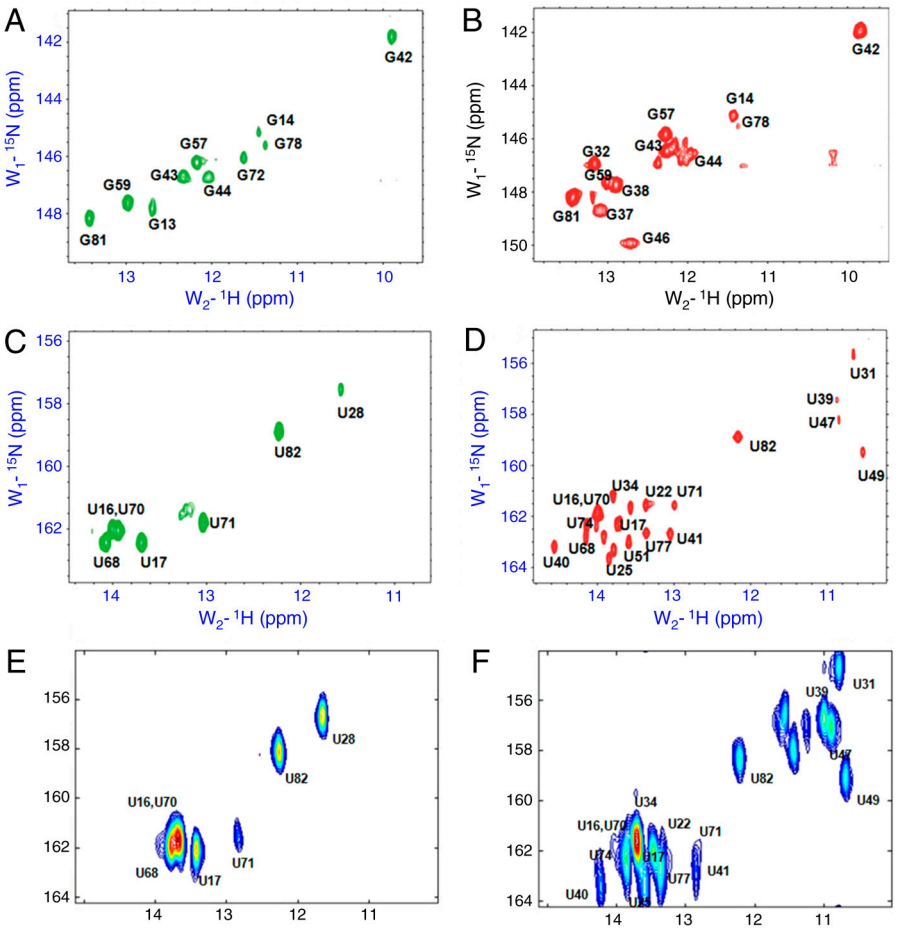

Fig. 2. Two-dimensional spectra of the ligand-free and ligand-bound adenine-sensing riboswitch aptamer domain. Conventional ^{1}H, ^{15}N-HSQCs of the free (*A*) and bound (*B*) ^{15}N-G-labeled RNA. Conventional ^{1}H, ^{15}N-HSQCs of the free (*C*) and bound (*D*) ^{15}N-U-labeled RNA. UltraSOFAST ^{1}H, ^{15}N correlation spectra of the free (*E*) and bound (*F*) ^{15}N-U-labeled RNA.

adenine–riboswitch complex displayed strong NOEs between the imino protons of U74 and U51 and the H2 of the bound adenine. The most interesting NMR signals arising from this complex correspond to the imino proton peaks of the G37 and G38 residues. These peaks indicate the formation of stable long-distance base pairs between G37 and C61, as well as G38 and C60. The appearance of the G37 and G38 imino proton peaks indicates that the interactions between loops 2 and 3 are formed successfully.

UltraSOFAST HMQCs of the A-Riboswitch Aptamer Domain. In order to establish our ability to collect multidimensional spectra for real-time NMR studies, ultraSOFAST ^{1}H, ^{15}N-HMQCs of [^{15}N-G]- or [^{15}N-U]-labeled riboswitches were recorded. As discussed more extensively elsewhere (18), these experiments combine the single-scan 2D NMR acquisition ability of spatially encoded methods (20) with the rapid-repetition abilities of longitudinally optimized schemes (21, 22) for the sake of achieving repetitive 2D NMR acquisition at very fast rates. However, at the concentrations available in this work (about 1 mM and involving rapid mixing of reactants), at least four single-scan 2D spectral acquisitions had to be coadded for achieving sufficient sensitivity; given the 0.3 sec repetition delays of each single scan, the minimal acquisition time ended up being ≈1.2 sec per 2D spectrum. For even better signal-noise, some of the data were averaged further by interleaving eight or more phase-cycled HMQC spectra, for a total 2D acquisition time of ~2.4. 4.8 or 9.6 sec. Although the imino peaks in the resulting ultrafast spectra are less well resolved compared to their conventional 2D spectra (Fig. 2 *E* and *F*), most ultraSOFAST resonances are resolved well enough to be unambiguously associated with peaks in the conventional HSQCs.

Fig. 3 illustrates representative changes observed as a function of time from the moment of injection in the real-time 2D NMR experiments for several Uracil bases whose signals changed upon injection of the ligand. After addition of the ligand by rapid mixing, signals corresponding to the free species decrease, while resonance stemming from the adenine-bound RNA increase over time. The appearance of a new peak indicates the formation of a new set of hydrogen bonds, stable enough to lead to protection from exchange with solvent. It is clear that peaks corresponding to the bound state of the RNA arise with different kinetics, that for convenience we classify into "slow," "intermediate," and "fast." Peaks with slow kinetics (like U49) can be analyzed at higher sensitivity by using progressively extended cycles of data averaging or even conventional 2D acquisition methods. Fig. 3 shows resonances that can only be followed using fast real-time acquisition techniques; some of the peaks (such as U22 and U71) arise so rapidly that even a 2.4 sec acquisition time is too long to follow the kinetics of their appearance. Altogether, these data provide a site-resolved picture of the various rearrangement steps undergone by the RNA during the conformational transition.

Conformational Transition of the Riboswitch in Real Time. Based on the assignments of the free and bound riboswitch spectra, we were able to assign the imino protons of a series of ultraSOFAST HMQCs recorded with a resolution of just a few seconds. Out of the multiple dynamic datasets that were recorded for this work, we focus on two representative experiments. In the first set of studies, the ligand was mixed manually outside the magnet with a G-enriched RNA; no spectra could be collected within the first 16 sec due to the need to manually insert the tube into the magnet (Fig. 4*A*). The second dataset was collected on a U-enriched sample using rapid injection inside the magnet with data recording already active; the initial dead time was in this second case much shorter, about 1 sec (Fig. 4*B*). The general features revealed by both sets of experiments were complementary and are as follows.

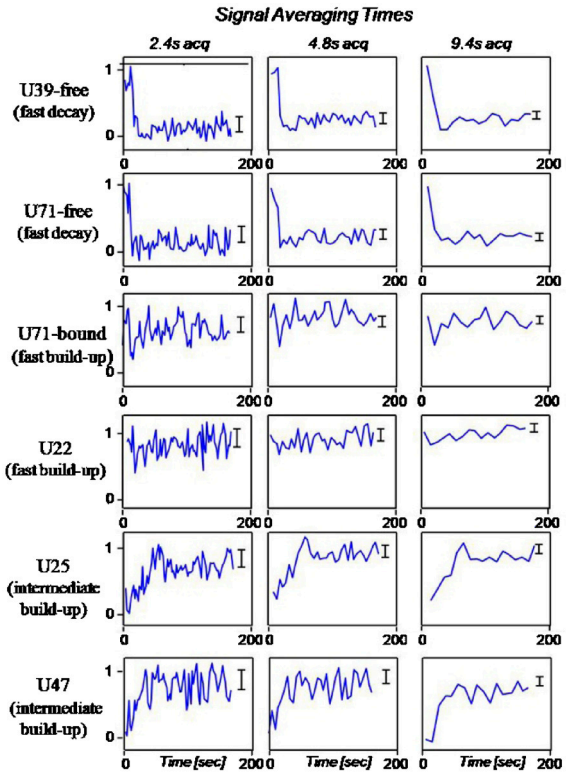

Fig. 3. Signal buildup and decay curves for representative sites in the riboswitch; different spectra are averaged together in the three set of data, corresponding to (left to right) time resolutions of 2.4, 4.8 and 9.6 sec. Plots cover the first 200 sec of the reaction and markers on the right of each plot denote the statistical noise spread (95% confidence limits) of each measurement.

Earliest time points (5–20 sec)—In the G-focused data, the imino proton peaks of G43 and G44 in the free RNA disappear and new peaks from the complex are observed after 16 sec (Fig. 4*A*, panel 16 sec). Interestingly, even though we could observe a stable G72 imino peak in the free RNA spectrum, this peak disappears in these initial spectra and is not observed even as a low intensity peak. Many new peaks appeared in the shortest spectra recorded on the U-labeled sample, even prior to 10 sec, which could be accessed because of more rapid injection. Among them are the U31 and U39 residues, located in P2 near Loop 2 (Fig. 1), which represent a U-U base pair in the bound structure. Other fast build-up peaks arise from residues U22 in J1-2, U47, U49, and U51 in J2-3, which are involved in the formation of the core structure required for ligand binding (Fig. 4*B*, panel 19.2 sec). In the P1 helix, signals corresponding to the U20 and U77 residues rapidly emerge indicating an extension of the P1 helix upon ligand binding. New peaks appear for U28 and U49, while the U71 peak corresponding to the free conformation (near G72) disappears from the spectrum, and its new bound-conformation counterpart appears. The residues that show changes in the 16 sec spectrum are distributed in all three of the helices (P1, P2, and P3), implying that ligand binding has already affected the entire RNA structure. Taken together, these results indicate partial formation of the core structure within just a few seconds after adenine binding, which stabilizes the three-way junction and part of the P1 helix.

Intermediate time regime (28–58 sec)—New imino peaks corresponding to G37, G38, G32, and G46 appear by 28 sec (Fig. 4*A*, panel 28 sec), indicating that the G37 and G38 residues in loop 2 form base pairs with C60 and C61 in loop 3 by this time. These base pairs are key features of the adenine–riboswitch complex. This loop-2/loop-3 interaction also stabilizes the G32 residue

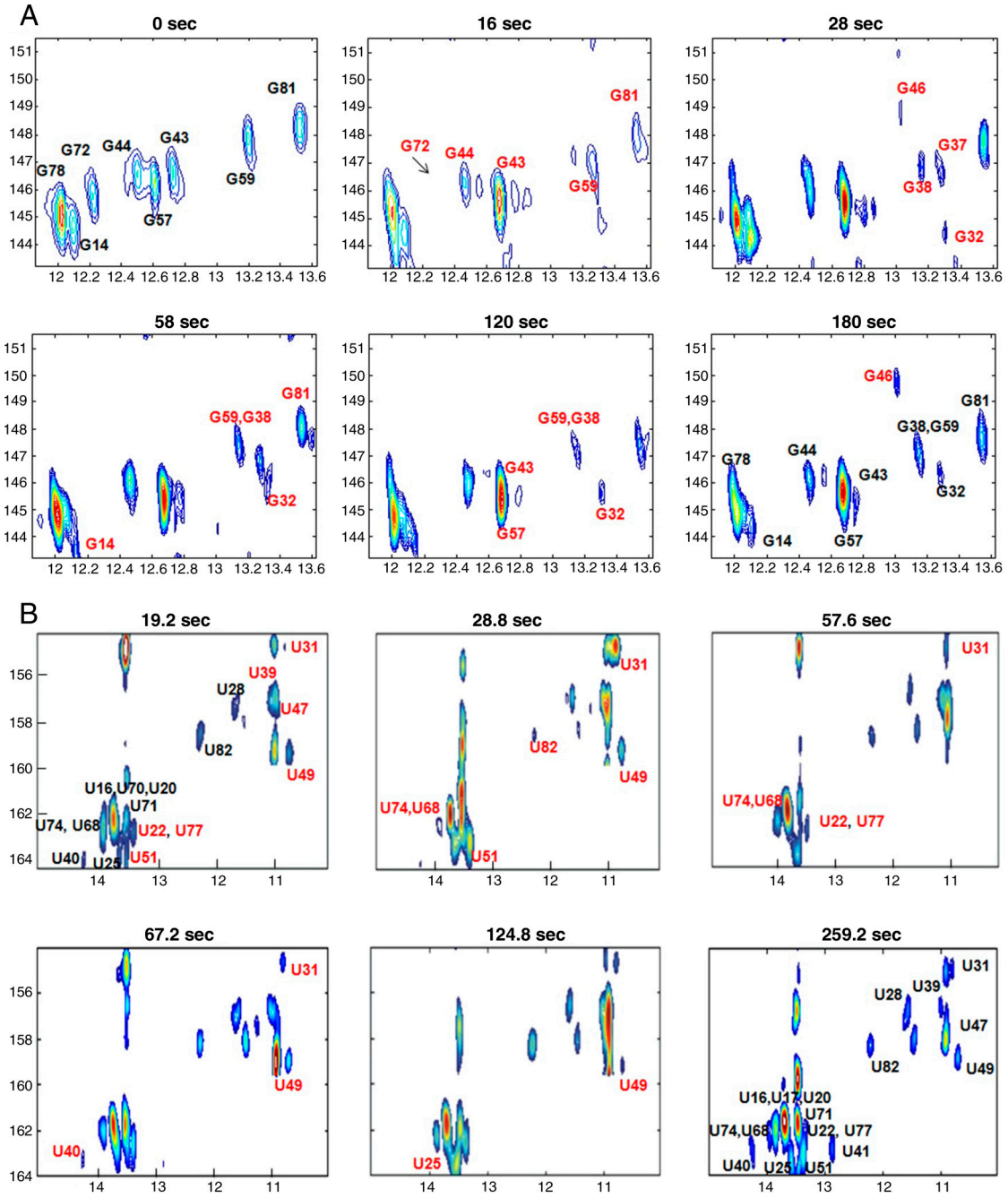

Fig. 4. (*A*) Representative real-time 2D HMQC NMR spectra recorded at pH 6.1 and 298 K on a ~1.7 mM ^{15}N-G-labeled adenine riboswitch ligand-binding domain; the times indicated in each frame correspond to the time point following addition of adenine and Mg^{2+} to the free RNA solution. (*B*) Representative real-time 2D HMQC spectra of the [^{15}N-U]-labeled riboswitch recorded at the indicated times following ligand addition in the magnet by rapid mixing. Spectral assignments are indicated on the figures.

in loop 2, leading to the appearance of its imino peak. The G46 base located near the ligand-binding core also appears at this point; although its intensity is low, this appearance demonstrates that the riboswitch has already started to build up its core structure by the ½-min time mark.

At longer times, close to the 48 sec time point, an interesting change in the U-spectra is given by the new U41 peak formed within P2 (Fig. 4*B*, panel 57.6 sec). Furthermore, most peaks are increased in intensity, except for U49 from J2-3. These changes suggest that all helices and loop structures have been stabilized at this stage by the adenine addition, except for the J2-3 region. The G spectrum recorded at *ca.* 1 min presents remarkably increased intensities for the G37, G38, and G32 peaks. This observation suggests that the interactions between loops 2 and 3 continue to be considerably stabilized vis-à-vis their status at shorter time intervals. By this time, the free RNA signal has essentially disappeared for most residues, with the exception of G81 and G14 in the terminus of the P1 helix, which show separate peaks corresponding to free and bound forms of the riboswitch. By 67 sec (Fig. 4*B*), the U-spectra show stabilized peaks from helices and loops, but most peaks are not yet at full intensity. This observation implies that even at this late stage the helices and loops have been stabilized, but the structural transition is not yet fully completed.

Long time regime (>120 sec)—About 3 min following adenine binding, most U and G peaks are present with high intensities (Fig. 4 *A* and *B*), indicating that a complete bound structure is fully formed. In particular, the G46 peak is dramatically increased in intensity compared to shorter time points. At the latest time points, the U spectra only undergo some subtle chemical shift changes compared to earlier time points, and all bound peaks are observed with high intensity. Interestingly, though, the tertiary interactions between loop 2 and loop 3 appear to be fully stabilized only over this relatively long time frame, leading to the very slow completion of the riboswitch structural rearrangement.

Discussion

The 71-nucleotide A-sensing riboswitch ligand-binding domain is an important example of biological regulation and a paradigmatic system to study RNA conformational transitions. It undergoes a dramatic change in its order and structure upon binding the substrate in the presence of Mg^{2+} ions. While the structure of the riboswitch and the molecular basis for substrate recognition are now clear (9–11), the conformational trajectories linking the two conformational states of the RNA are only partially characterized. Completing this task constitutes an important challenge because of its general importance to understanding RNA folding and because riboswitch activity appears to be regulated kinetically through a competition between the rates of the conformational transition and of polymerase elongation.

The pathways by which the conformational change occur have been followed in real time using single molecule techniques while the RNA was still attached to the polymerase (14) and by 1D-NMR combined with photodissociation strategies (12). These real-time NMR experiments enabled the determination of kinetic rates for conformational transitions of some individual residues during ligand-induced RNA folding, and the identification of intermediate states along the conformational pathways, but many residues were inevitably overlapped and had to be analyzed in clusters or could not be analyzed at all. The present study shows that, with the aid of emerging multidimensional NMR spectroscopy methods, it is possible to follow and to extend these characterizations of RNA conformational transitions in real time, with a resolution of a few seconds. These techniques also open the possibility to determine the structures and dynamics of intermediates along the pathways through the collection of other observables, like residual dipolar couplings and/or relaxation–dispersion curves (23, 24), that require the spectral resolution of 2D NMR.

The real-time 2D NMR measurements described in this study allowed us to describe the conformational transition of the adenine-sensing riboswitch using a sequential model. Identifiable intermediates correspond to the formation of the ligand-binding pocket (Fig. 5*B*) and the formation (Fig. 5*C*) and stabilization (Fig. 5*D*) of tertiary loop–loop interactions that stabilize the bound structure of the riboswitch. Previous NMR studies based on 1D NMR methods had suggested that binding of the ligand occurred with a rate of about 20 sec and that tertiary base pairs form with a slightly slower rate (12). Our observations for the early-to-intermediate time scales are consistent with these results, although many resonances could not be observed by 1D NMR. As suggested in the single molecule optical tweezer study, helix P1 is only partially formed in the free state and full stabilization does not occur until the entire structure is fully formed 2–3 min after addition of the ligand. In the remainder, we describe in detail the most salient spectral observations.

At the earliest time points investigated (~15 s, Figs. 4 and 5*B*), the spectra exhibit a number of peaks corresponding to the bound conformation of the riboswitch, but many peaks are also broadened by conformational exchange. Residues from the core overlapped in the 1D NMR study are well separated in the 2D NMR spectra and can be confidently identified in the present study.

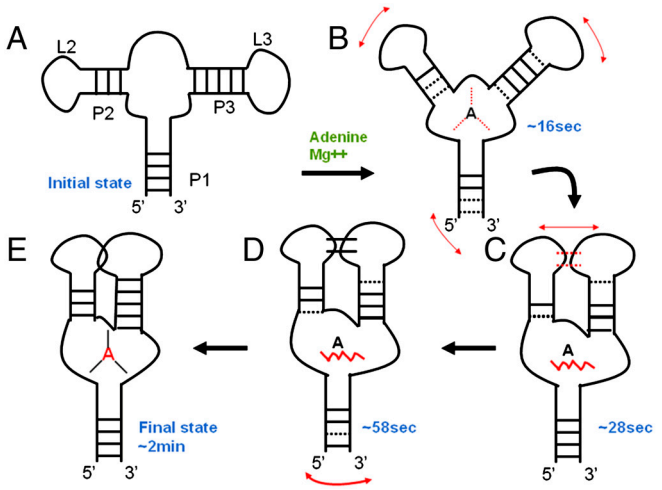

Fig. 5. Secondary structure representation of the ligand-induced folding of the adenine-sensing riboswitch ligand-binding domain, as revealed by real-time 2D NMR. Dotted lines and zigzag symbols indicate unstable hydrogen bonding and flexible structural features, respectively. (*A*) Free conformation of the riboswitch; helices P2 and P3 are formed, but P1 is only partially stable, as also observed by single molecule measurements (14); (*B*) Formation of the ligand-binding pocket occurs rapidly, with a rate (16 sec) comparable to the 1D NMR observation (12), but helix P1 remains partially unfolded (14); (*C*) Tertiary contacts between loop 2 and 3 are observed after the formation of the ligand-binding pocket; and (*D*) they are fully stabilized after approximately 1 min, though structural flexibility is retained in helix P1. (*E*) Formation of the final bound structure is completed after 2–3 min.

Some base pairs (e.g., G14-U82 and C18-G78) are preserved throughout these early events, but new base pairs corresponding to the final complex begin to appear (e.g., U20-A76 and A21-U77). Unexpectedly, a number of base pairs within helices P2 and P3 (G43-C27, G44-C26, and G59-C67) become unstable and new, transient base-pairs form, suggesting that helices P2 and P3 may transiently unfold during the formation of the tertiary interactions. The observation of new peaks corresponding to U22, U47, U51, and U74 implies that the initial interactions between the riboswitch central core and adenine begin to form very fast following ligand addition, consistent with the formation of the ligand-binding pocket observed by 1D NMR with rates of 19–24 sec (12).

Long range interactions between loop 2 and loop 3 begin to form about 30 sec following addition of the ligand (Fig. 5*C*), although the weak intensity of the peaks suggests that these base pairs are only partially stabilized (Fig. 4). The appearance of both the G37 and G38 imino proton peaks in the spectra demonstrates the initial formation of both the G37-C61 and G38-C60 base pairs observed in the structure of the complex (9, 10). Even if adenine is clearly bound to the central core structure, the conformation of the riboswitch remains unstable, as evidenced by the very weak imino peak of G46 located in this central region (Fig. 4*A*).

Stronger interactions between loop 2 and loop 3, and the stabilization of the base pairs in the P2 and P3 helices, occurs after about 50 sec (Fig. 5*D*). Timescales for this process were measured by 1D NMR to be 27–30 sec, consistent with the near completion of this process revealed by real-time 2D NMR after 60–90 sec (Fig. 4). However, the terminal part of the P1 helix and the central core are not fully formed yet: The riboswitch ligand-binding core and the riboswitch tertiary structure have not yet fully stabilized. The 1D real-time NMR study also reported a slower process for the full stabilization of nucleotides within helices P2 and P3 and of the loop2–loop3 interactions (12), while the single molecule study concluded that formation of the secondary structure (but not of helix P1) preceded the stabilization of the core. The final stabilization of the central core and formation of the

final structure of the riboswitch occurs over >2 minutes (Figs. 4 and 5*E*): Only after 180–240 sec are all the imino proton peaks present in the standard ^{1}H, ^{15}N-HSQCs also observed in the spectra with full intensity.

In the free riboswitch, there are only seven visible signals among 24 possible U imino protons, suggesting that its structure is unstable and dynamic. Other NMR data demonstrate that the P2 and P3 helices of the free riboswitch are relatively stable, yet the helical junction and part of the P1 helix remain flexible even if the bases retain helical stacking. In the *add* adenine-sensing riboswitch with both aptamer and expression platform domains, one strand of the P1 helix is believed to be involved in the formation of the translation repressive structure with part of expression platform domain in the absence of ligand (25). In our adenine-binding study, the P1 helix was extended and stabilized even at the earliest time point observed (10–15 sec), yet remain partly unstable until the complete structure is formed. These observations suggest that adenine binding promotes rapid P1 helix formation in competition between the P1 helix and the repressor stem in the expression platform of full-length riboswitch domain.

In summary, by recording time-resolved 2D NMR spectra with resolutions of a few seconds we have followed in real time the formation of hydrogen bonds between the ligand and the riboswitch and within the riboswitch. The real-time monitoring of the folding process by multidimensional NMR demonstrates that it is possible to study folding transitions in RNA when kinetics are in this timescale. We are confident that, by further optimizing the sensitivity of these 2D NMR methods and by combining them with additional experimental approaches (such as residual dipolar coupling measurements), it will become possible to generate sufficient structural information to map the conformational intermediates with even higher temporal resolution and with structural detail.

Materials and Methods

RNAs were prepared using the T7 RNA polymerase method, as detailed in *SI Text*. Complete spectral assignments for the base HN and HC protons, as well as ribose H1′ and H2′ protons, were obtained using highly deuterated samples that were only protonated at the desired positions to minimize spectral overlap and linewidth (19). The ultraSOFAST real-time 2D NMR experiments were collected on Bruker DRX-800 MHz NMR spectrometer utilizing a triple-tuned TXI single-gradient cryogenic probe at 298 K. Riboswitch folding was triggered using a custom-made device injecting ~90 μL of a solution containing adenine and $MgCl_2$, into a 5 mm Shigemi tube containing ~500 μL of a potassium phosphate buffered sample that already included the ^{15}N-labeled RNA. Following injection, final nucleotide and $MgCl_2$ concentrations were ~1 and 10 mM, respectively, whereas the final RNA concentrations ranged between 0.9–1.8 mM in different experiments. The relatively large initial solution volume waiting in the pretuned, preshimmed 5 mm tube environment allowed for a relatively stable shimming upon injecting the ligand. As a result, constant 2D peak amplitudes could be repetitively measured about ~1 sec following the nucleotide's injection; data collection had already been initiated prior to injection. The pulse sequence chosen for these real-time 2D tests was based on the ultraSOFAST HMQC experiment (18) with the modifications described in *SI Text*. The sensitivity afforded by the minimal two-scan phase cycling demanded by water-suppression considerations on the ~1 mM solutions investigated in this study was not always sufficient for unambiguous quantification of the riboswitch kinetics. Thus, data from two consecutive phase-cycled experiments were generally interleaved. Given the 300 ms repetition times between scans, each HMQC dataset acquisition required a minimum of 1.2 sec per 2D experiment. The resulting NMR datasets were processed into 2D spectra and analyzed using custom-written Matlab scripts.

ACKNOWLEDGMENTS. L.F. acknowledges support for this research by the Israel Science Foundation (ISF 447/09), the European Commission (EU-NMR contract No. 026145), a Helen and Kimmel Award for Innovative Investigation, and by the generosity of the Perlman Family Foundation. G.V. acknowledges support of an National Institutes of Health National Institute of Biomedical Imaging and Bioengineering grant.

1. Winkler WC, Breaker RR (2005) Regulation of bacterial gene expression by riboswitches. *Annu Rev Microbiol* 59:487–517.
2. Leulliot N, Varani G (2001) Current topics in RNA-protein recognition: Control of specificity and biological function through induced fit and conformational capture. *Biochemistry* 40:7947–7956.
3. Williamson JR (2000) Induced-fit in RNA-protein recognition. *Nature Struct Mol Biol* 7:834–837.
4. Mandal M, Breaker RR (2004) Gene regulation by riboswitches. *Nat Rev Mol Cell Biol* 5:451–63.
5. Soukup JK, Soukup GA (2004) Riboswitches exert genetic control through metabolite-induced conformational change. *Curr Opin Struct Biol* 14:344–9.
6. Wickiser JK, Chea MT, Breaker RR, Crothers DM (2005) The kinetics of ligand binding by an adenine-sensing riboswitch. *Biochemistry* 44:13404–13414.
7. Wickiser JK, Winkler WC, Breaker RR, Crothers DM (2005) The speed of RNA transcription and metabolite binding kinetics operate an FMN riboswitch. *Mol Cell* 18:49–60.
8. Gilbert SD, Stoddard CD, Wise SJ, Batey RT (2006) Thermodynamic and kinetic characterization of ligand binding to the purine riboswitch aptamer domain. *J Mol Biol* 359:754–768.
9. Batey RT, Gilbert SD, Montange RK (2004) Structure of a natural guanine-responsive riboswitch complexed with the metabolite hypoxanthine. *Nature* 432:411–415.
10. Serganov A, et al. (2004) Structural basis for descriminative regulation of gene expression by adenine- and guanine-sensing mRNAs. *Chem Biol* 11:1729–1741.
11. Noeske J, et al. (2005) An intermolecular base triple as the basis of ligand specificity and affinity in the guanine- and adenine-sensing riboswitch RNAs. *Proc Natl Acad Sci USA* 102:1372–1377.
12. Buck J, Furtig B, Noeske J, Wohnert J, Schwalbe H (2007) Time-resolved NMR methods resolving ligand-induced RNA folding at atomic resolution. *Proc Natl Acad Sci USA* 104:15699–15704.
13. Noeske J, Schwalbe H, Wohnert J (2007) Metal-ion binding and metal-ion induced folding of the adenine-sensing riboswitch aptamer domain. *Nucleic Acids Res* 35:5262–73.
14. Greenleaf WJ, Frieda KL, Foster DAN, Woodside MT, Block SN (2008) Direct observation of hierarchical folding in single riboswitch aptamers. *Science* 319:630–633.
15. Lemay J-F, Penedo JC, Tremblay R, Lilley DMJ, Lafontaine DA (2006) Folding of the adenine riboswitch. *Chem Biol* 13:857–868.
16. Kupce E, Freeman R (2008) Hyperdimensional NMR spectroscopy. *Prog Nucl Mag Res Sp* 52:22–30.
17. Mishkovsky M, Frydman L (2009) Principles and progress in ultrafast multidimensional nuclear magnetic resonance. *Annu Rev Phys Chem* 60:429–448.
18. Gal M, Schanda P, Brutscher B, Frydman L (2007) UltraSOFAST HMQC NMR and the repetitive acquisition of 2D protein spectra at Hz rates. *J Am Chem Soc* 129:1372–1377.
19. Scott LG, Tolbert TJ, Williamson JR (2000) Preparation of specifically 2H- and 13C-labeled ribonucleotides. *Methods Enzymol* 317:18–38.
20. Frydman L, Scherf T, Lupulescu A (2002) The Acquisition of multidimensional NMR spectra within a single scan. *Proc Natl Acad Sci USA* 99:15858–15862.
21. Pervushin K, Voegeli B, Eletsky A (2002) Longitudinal 1H relaxation optimization in TROSY NMR spectroscopy. *J Am Chem Soc* 124:12898–12902.
22. Schanda P, Brutscher B (2005) Very fast two-dimensional NMR spectroscopy for real-time investigation of dynamic events in proteins on the time scale of seconds. *J Am Chem Soc* 127:8014–8015.
23. Palmer AGI, Kroenke CD, Loria JP (2001) Nuclear magnetic resonance methods for quantifying microsecond-to-millisecond motions in biological macromolecules. *Method Enzymol* 339:204–238.
24. Mulder FAA, Mittermaier A, Hon B, Dahlquist FW, Kay LE (2001) Studying excited states of proteins by NMR spectroscopy. *Nat Struct Biol* 8:932–935.
25. Rieder R, Lang K, Graber D, Micura R (2007) Ligand-induced folding of the adenosine deaminase A-riboswitch and implications on riboswitch translational control. *Chembiochem* 8:896–902.